research papers

Complete polarization analysis of an APPLE II undulator using a soft X-ray polarimeter

Hongchang Wang,[a]* Peter Bencok,[a] Paul Steadman,[a] Emily Longhi,[a] Jingtao Zhu[b] and Zhanshan Wang[b]

[a]Diamond Light Source, Didcot OX11 0DE, UK, and [b]Key Laboratory of Advanced Micro-structured Materials, MOE, Institute of Precision Optical Engineering, Department of Physics, Tongji University, Shanghai 200092, People's Republic of China. E-mail: hongchang.wang@diamond.ac.uk

Two APPLE II undulators installed on the Diamond I10 beamline have all four magnet arrays shiftable and thus can generate linear polarization at any arbitrary angle from $0°$ to $180°$, as well as all other states of elliptical polarization. To characterize the emitted radiation polarization state from one APPLE II undulator, the complete polarization measurement was performed using a multilayer-based soft X-ray polarimeter. The measurement results appear to show that the linear polarization angle offset is about $6°$ compared with other measurements at 712 eV, equivalent to an undulator jaw phase offset of 1.1 mm. In addition, the polarization states of various ellipticities have also been measured as a function of the undulator row phase.

1. Introduction

Undulators are in high demand at modern synchrotron radiation facilities since they can provide several orders of magnitude higher flux than a simple bending magnet. Meanwhile, the polarization of the emitted radiation can be controlled freely by using the relative position of the permanent magnets to induce different periodic electron trajectories through the undulator. This variable polarization has received increasing interest for the study of a wide range of phenomena in biology, chemistry, physics and materials science. Since the 1990s, various polarization features of undulators with different phasing modes have been proposed and developed (Hwang & Yeh, 1999). Among them, APPLE-II-type elliptically polarized undulators (EPUs) are widely used owing to their flexibility in varying the polarization state between arbitrary linear polarization, left- and right-handed circular polarization by adjusting the magnetic arrays (Sasaki, 1994; Lidia & Carr, 1994). In principle, the polarization state of radiation from an undulator can be derived once the magnetic field has been calculated using numerical techniques (Chubar et al., 1998). However, many factors, such as the non-uniformity of the magnetic field along the undulator, small offsets among the magnetic arrays and the beamline optics, can change the polarization state at the end-station from that predicted in the theoretical calculation. Furthermore, in many synchrotron sources, X-rays from higher harmonics of the insertion device are used, for which the polarization, in the case of circular light, is not expected to be 100%. In some cases, two undulators will be required to switch the polariza-tion promptly (Weiss et al., 2001). Therefore, it is essential to measure the precise polarization state at the sample location from both devices. In addition, it is also important to learn about the symmetry between the left- and right-handed circular polarization for some polarization-dependent experiments.

In the last two decades the polarization state of synchrotron radiation from various undulators has been characterized using different types of polarimeters in the vacuum ultraviolet region (Carr et al., 1995; Drescher et al., 1997; Weiss et al., 2001; Nahon & Alcaraz, 2004; Bahrdt et al., 2010). The X-ray absorption spectrum of an oriented polytetrafluoroethylene thin film was also used to exhibit the variable linear polar-ization capability of an APPLE II EPU (Young et al., 2002). The previous study showed that the polarization measurement can assist in compensating the beamline polarization owing to the depolarization effects from beamline optics (Bahrdt et al., 2010). Owing to the lack of suitable phase retarders, some polarization measurements only employed a simple Rabino-vitch-type polarimeter, but the depolarization cannot be distinguished from circular polarization in this case (Carr et al., 1995; Weiss et al., 2001). In one case the complete polarization analysis for an APPLE II undulator was carried out at 95 eV using an aperiodic Mo/Si multilayer (Wang et al., 2007a), and the asymmetric effect for the linear component was noted. The free-standing W/B_4C multilayer has been proved to be suitable as a phase retarder at photon energies between 700 eV and 1000 eV, but the complete polarization analysis was only demonstrated for the single elliptical and linear polarization (MacDonald et al., 2009).

Several beamlines at Diamond Light Source (DLS) are equipped with APPLE II undulators capable of providing variable polarization, which are greatly beneficial to many polarization-sensitive experiments such as angle-resolved photoemission, studies of magnetic linear and circular dichroism, scanning transmission X-ray microscopy and inelastic X-ray scattering. Knowledge of the degree of polarization is vital, not only for understanding the undulator or beamline performance but also to carry out precise analysis of experiments in order to understand material properties. Hence, a dedicated soft X-ray polarimeter was recently developed for accurately characterizing the polarization performance of these beamlines (Wang *et al.*, 2011). For this paper, one APPLE II undulator was operated in both the linear arbitrary mode and elliptical polarization mode, and the variable polarization states of the emitted radiation from the undulator were fully characterized at 712 eV using the multilayer-based polarimeter.

2. APPLE-II undulator

Two identical undulators were installed on beamline I10 at DLS. They each have 40 full-size periods with period length λ_u of 48 mm, and the schematics of one of the APPLE II undulators are demonstrated in Fig. 1. The minimum gap is 16 mm and the maximum deflection factor in horizontal mode is 3.49. The undulators are able to produce arbitrary linear and circularly polarized light from 500 to 1700 eV on the first harmonic. In the fast polarization switching mode, each undulator is set to one of the two polarizations that are required (for example, left-handed circular for one undulator and right-handed circular for the other undulator) (Bahrdt *et al.*, 2001; Quitmann *et al.*, 2001; Schmidt & Zimoch, 2007). Instead of seven steerer magnets used at the Swiss Light Source (Quitmann *et al.*, 2001), two magnets are placed before the two undulators and two afterwards, and the remaining kicker magnet is placed in the centre. The five fast-switching chicane magnets effectively select which undulator's light passes through the beamline aperture, and it allows rapid switching between polarizations at up to 10 Hz. In this experiment the upstream undulator gap was fully open, so that only the downstream undulator was used to generate various polarization states.
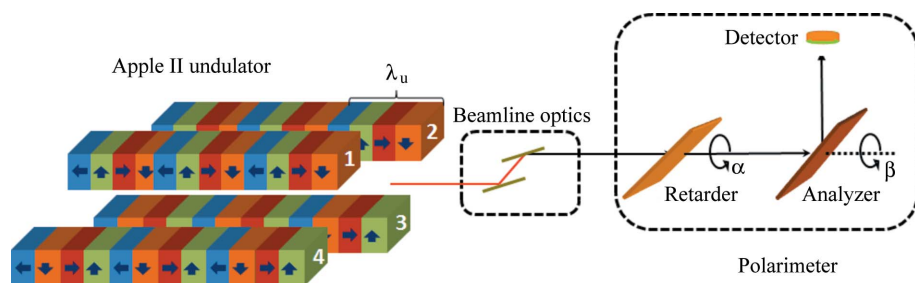
The undulators installed on I10 have four movable magnet arrays and a variable undulator gap. Thus all polarization modes and energies are accessible. The analytical description of this APPLE II undulator operation was presented by Schmidt & Zimoch (2007). Moving diagonally opposed arrays in the same direction (such as $s_1 = s_3$) with respect to each other changes the polarization from linear horizontal ($s_1 = s_3 = 0$) through elliptically polarized and circularly polarized to linear vertical ($s_1 = s_3 = \lambda_u/2$). If the diagonal arrays are moved in opposition ($s_1 = -s_3$), then linear polarization with a variable angle between $0°$ and $180°$ can be produced. The amount that the arrays can be moved, defined as the row phase, is variable from 0 mm up to half a period, $\lambda_u/2 = 24$ mm, in either direction. The energy can be controlled by changing the gap, or can be controlled by a simultaneous shift of the two upper magnet arrays (1 and 2) with respect to the two lower magnet arrays (3 and 4). This movement is defined as the jaw phase. A new high-symmetry mode has also been used to control the energy and the polarization angle (Schmidt & Zimoch, 2007). In this case the undulator gap is used to change the energy and the polarization angle is linearly dependent on the jaw phase.

Regarding the beamline optics, a collimated plane-grating monochromator is used for the I10 beamline. This gives flexibility to operational modes of the beamline such as being able to operate in either high-resolution mode or high-harmonic-suppression mode. The grating line density is 400 lines mm^{-1} and gold coatings were used for both mirrors and grating. The depolarization effect from beamline optics can be neglected at the working energy since the grazing angles for the mirrors and grating are less than $1.5°$.

To gain precise knowledge of the polarization state of the emitted synchrotron radiation from the above undulator a high-precision polarimeter was required to provide a precise and complete polarization analysis of the synchrotron radiation at the sample location. In the case of soft X-ray polarimetry the alignment requirements between the polarimeter and incident photon beam are very stringent since the multilayer bandwidth is usually a few milliradians or even less. The high-precision polarimeter was supported on a hexapod to simplify the angular alignment with resolution better than 5 µrad (Wang *et al.*, 2011). It contains a transmission multilayer phase retarder and a reflection multilayer analyzer. A photodiode detector was used to collect the transmitted signal through polarizing elements by rotating both the retarder (α) and analyzer (β) independently about the optical axis of the beam, and the schematics of the polarimeter are also illustrated in Fig. 1.

3. Complete polarization analysis

The polarization of the light is described by the Stokes parameters: S_0 (total intensity), S_1 (linear polarization), S_2 (linear polarization in a plane rotated by $45°$ with respect to the S_1 plane) and S_3 (circular polarization) (Koide *et al.*,

Figure 1
Schematics of the APPLE II undulator and polarimeter.

Table 1
Multilayer parameters for the phase retarder and analyzer used in the polarimetry experiment at 712 eV.

	Retarder	Analyzer
Multilayer	W/B$_4$C	W/B$_4$C
Periodic number N	320	250
Periodic thickness d [nm]	1.7	1.24
W thickness ratio $\Gamma = d_W/d$	0.236	0.35
Working angle θ (°)	30.2	44.8
R_s or T_s (%)	1.0	2.6
R_p or T_p (%)	1.1	0.001

1991; Schäfers *et al.*, 1999; Nahon & Alcaraz, 2004). Since the full polarization is a self-calibrating measurement, the Stokes parameters normalized with respect to the total intensity S_0 are defined as Stokes–Poincaré parameters with $P_i = S_i/S_0$ (Koide *et al.*, 1991). These parameters can be given by

$$\begin{cases} P_1 = (E_p{}^2 - E_s{}^2)/(E_p{}^2 + E_s{}^2), \\ P_2 = 2E_pE_s\cos(\varphi_s - \varphi_p)/(E_p{}^2 + E_s{}^2), \\ P_3 = 2E_pE_s\sin(\varphi_s - \varphi_p)/(E_p{}^2 + E_s{}^2). \end{cases} \quad (1)$$

Here E_s and E_p are the vertical and horizontal components of the electric field, and φ_s and φ_p denote the perpendicular and parallel phases of the polarized light to the plane of incidence. If the two electric field components E_s and E_p are equal, and the phase shift $\Delta\varphi = \varphi_s - \varphi_p$ is 90°, the polarization is defined as the right-handed circular polarization with $P_3 = 1$. To an observer looking in the direction from which the light is propagated, the electric vector would appear to describe a clockwise ellipse for the right-handed circular polarization.

In order to perform a complete polarization analysis of light, one needs both a retarder to introduce phase retardation between the two electric field components and an analyzer that transmits preferably only one particular linearly polarized component. For the complete polarization in the soft X-ray region the multilayer optical elements have been well developed as transmission phase retarders and reflection analyzers (Kortright & Underwood, 1990; Schäfers *et al.*, 1999; MacDonald *et al.*, 2009; Kimura *et al.*, 1995, 2005; Hirono *et al.*, 2005; Wang *et al.*, 2006, 2007*b*). The multilayer parameters used in this polarimetry experiment are listed in Table 1 (Wang *et al.*, 2011). For the multilayer analyzer the maximum polarizing power R_s/R_p between the s-component reflectivity R_s and p-component reflectivity R_p occurs at the quasi-Brewster angle near 45°. The periodic thickness d of the multilayer was chosen to be 1.24 nm according to the solution of the Bragg equation at the working energy of 712 eV. The measured reflectivity R_s and R_p is 2.6%

and 0.001%, respectively, at 712 eV. A free-standing W/B$_4$C transmission multilayer was used as a phase retarder at 30.2° grazing angle of incidence. This geometry was chosen since the roughness effects will decrease by operating the multilayers at lower grazing angles of incidence (Kimura *et al.*, 2005). The s-component transmission T_s and phase shift Δ of this multi-layer at 712 eV is 1.0% and −17°, respectively.

The detected light intensity I can be expressed as

$$\begin{aligned} I = F\Big\{ &\Big[1 + \cos 2\psi_1 \cos 2\psi_2 \cos 2(\alpha - \beta) \Big] \\ &+ P_1 \Big[\cos 2\alpha \cos 2\psi_1 \\ &+ \frac{1}{2}(1 + \sin 2\psi_1 \cos \Delta) \cos 2\psi_2 \cos 2\beta \\ &+ \frac{1}{2}(1 - \sin 2\psi_1 \cos \Delta) \cos 2\psi_2 \cos(4\alpha - 2\beta) \Big] \\ &+ P_2 \Big[\sin 2\alpha \cos 2\psi_1 \\ &+ \frac{1}{2}(1 + \sin 2\psi_1 \cos \Delta) \cos 2\psi_2 \sin 2\beta \\ &+ \frac{1}{2}(1 - \sin 2\psi_1 \cos \Delta) \cos 2\psi_2 \sin(4\alpha - 2\beta) \Big] \\ &+ P_3 \Big[\sin 2\psi_1 \cos 2\psi_2 \sin \Delta \sin 2(\alpha - \beta) \Big] \Big\}. \end{aligned} \quad (2)$$

Here, $\tan \psi_1 = (T_p/T_s)^{1/2}$, $\tan \psi_2 = (R_p/R_s)^{1/2}$, and T_p and T_s are the p- and s-component transmission for a multilayer phase retarder. The scale factor F is used to adjust the scale of the recorded intensity in the self-calibrating measurements.

Fig. 2 shows the measured intensity as a function of both the retarder rotation α and the analyzer rotation β for linear arbitrary angle χ at (*a*) 0°, (*b*) 45° and (*c*) 90°. Here there are
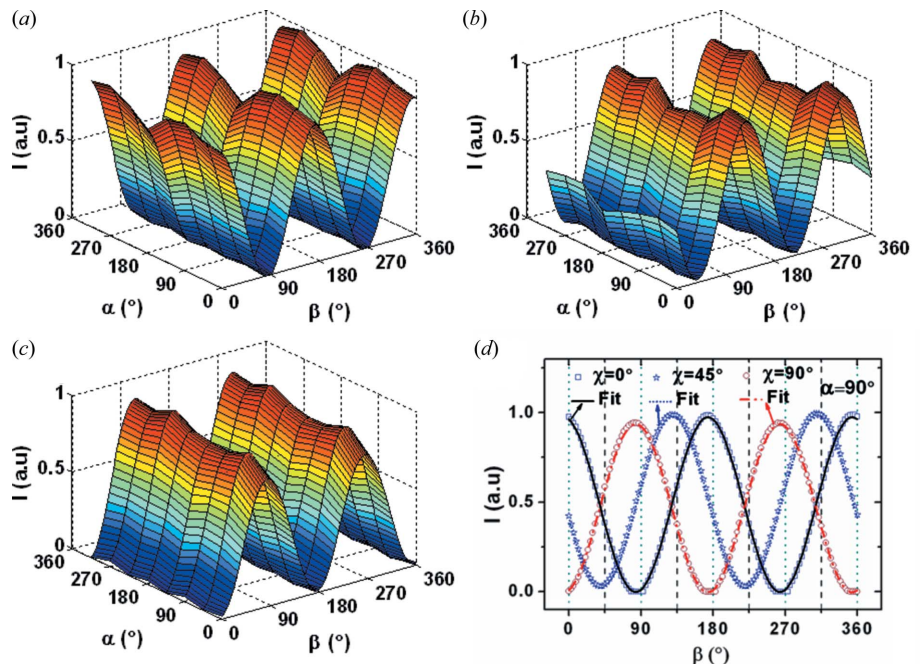
Figure 2
Measured intensity as a function of both the retarder rotation α and analyzer rotation β for three linear arbitrary angles χ: (*a*) 0°, (*b*) 45° and (*c*) 90°. (*d*) Measured and fitted intensity as a function of the analyzer rotation β for linear arbitrary angles of 0°, 45° and 90° at $\alpha = 90°$.

eight settings of α from 0° to 315° and 121 settings of β from 0° to 360° for one polarization scan. Fig. 2(d) is the measured and fitting intensity as a function of the analyzer rotation β for linear arbitrary 0°, 45° and 90° at $\alpha = 90°$. A least-squares method was used for fitting of measured data with equation (2), and both the Stokes–Poincaré parameters and the optics properties can be derived simultaneously. It can be noticed from Fig. 2(d) that the data are symmetric with respect to β, which proves that the analyzer rotation axis β is well aligned along the incident beam. Furthermore, the peak of the 'sine curve' shifts the equivalent angles as the linear polarization rotates from 0° to 45° and 90°. It also shows that there is an offset between peak position with the expected analyzer rotation angle β. For example, the maximum intensity should occur at 0° for $\chi = 0°$. Therefore, this result indicates that the arbitrary linear polarized light might not be well calibrated. This part will be addressed in the following section.

4. Polarimetry results

The diagonal arrays were firstly moved in antiphase with respect to each other ($s_1 = -s_3 = 15.4$ mm), and the linear arbitrary polarization angle χ can vary from 0° to 150°. The gap between the top row phase and bottom row phase is fixed at 17.412 mm to keep the energy at 712 eV. The jaw phase η was changed to tilt the polarization angle χ. The polarization angle was previously calibrated using the analyzer mounted in the RASOR diffractometer (Beale *et al.*, 2010), which is one of the permanent endstations on beamline I10. The measured Stokes–Poincaré parameters of the undulator radiation with η as a function of χ using the soft X-ray polarimeter are shown in Fig. 3. The jaw phase η depends linearly on the linear polarization angle χ with a slope of 0.13 mm per degree. This can only be moved from $-\lambda_u/4$ to $\lambda_u/4$. Therefore, once the required travel range for η is larger than one-quarter of an undulator period, then η has to subtract $\lambda_u/2$. The linear

polarization P_1 is 98.0% at $\chi = 0°$, and it decreases to -99.9% as the linear polarization angle χ changes to 90°; then it increases again as χ increases from 90° to 180°. Meanwhile, the polarization P_2 (linear polarization in a plane rotated by 45° with respect to the P_1 plane) reaches the minimum and maximum close to 45° and 135°, respectively. However, it clearly shows that there is an offset compared with the measured polarization (symbols) with the measured values using RASOR (solid lines), and the angular offset is around 6° from the fitting. In other words the measured polarization angle χ is 6° off compared with that measured using RASOR for linear horizontal polarization. The corresponding jaw phase offset is 1.1 mm. After shifting the curve (solid line) by 6° the measured polarization results agree well with the theoretical curve (dashed lines). It also confirms that the slope of linear fitting for η and χ is correct, and only the intercept has to be corrected with the offset of 1.1 mm.

The undulator row phase μ was then changed by altering the diagonally opposite arrays into the same direction ($s_1 = s_3$) with respect to each other in order to change the polarization state between the left-handed circular (lc), right-handed circular (rc), linear horizontal (lh) and linear vertical (lv) polarization. The measured Stokes–Poincaré parameters together with the jaw phase η as a function of the undulator row phase μ are shown in Fig. 4. The above polarizations are indicated by the dotted lines. The linear polarization component P_1 varies from 100.1% to -99.3% linear vertical when the top and bottom row phase change together from 0 to $\lambda_u/2$. The measured circular polarization P_3 at rc and lc are 100.5% and -99.9%, respectively. The linear Stokes–Poincaré parameter P_1 is 5% and 2% for rc and lc polarization, respectively. In addition, we note that the unpolarized light rate is less than 1% for the above measurement indicating that the non-zero emittance effects and magnetic inhomogeneities of the insertion device can be neglected.

Furthermore, the circular component P_3 varies from -3% to 4% for the linear polarization cases in Fig. 3, and the linear component P_2 varies from 2% to 3% for all datasets in Fig. 4,
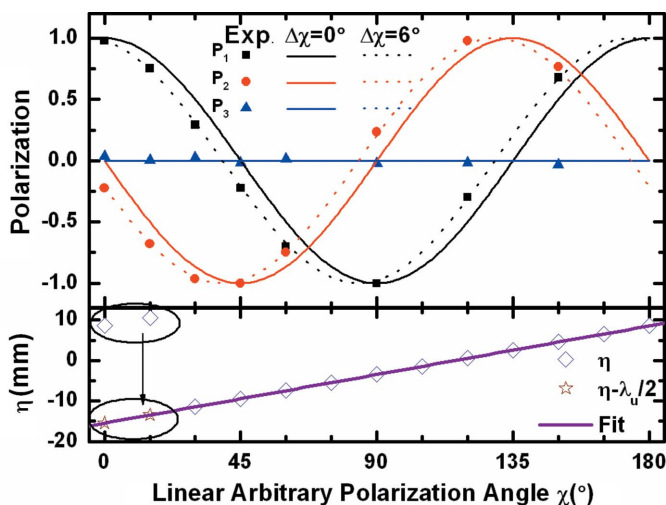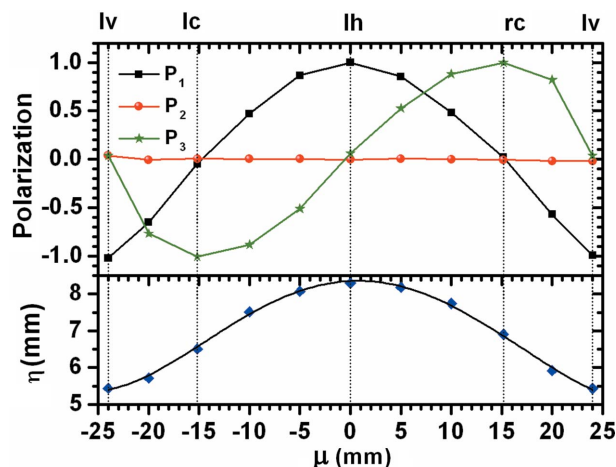

Figure 3
Measurement of the Stokes–Poincaré parameters of the undulator radiation and the jaw phase η values as a function of the linear arbitrary polarization angle χ for the first harmonic at 712 eV photon energy.

Figure 4
Measurement of the Stokes–Poincaré parameters of the undulator radiation and the jaw phase η values as a function of the undulator row phase μ for the first harmonic at 712 eV photon energy.

which means that the phase shift between E_p and E_s is not precisely 90°. The estimated uncertainty in each Stokes–Poincaré parameter is ±1% (Wang *et al.*, 2011, 2012). Various sources can contribute to the contamination of either linear or circular polarization components such as undulator end effects, or small deviations between the beam and polarimeter rotation axes at these energies. Therefore further tests will be required to address this issue in the near future.

5. Summary and future work

An APPLE II undulator has provided variably polarized beam by adjusting the four magnet arrays. The polarization states were accurately measured using a soft X-ray polarimeter with a W/B$_4$C multilayer phase retarder and analyzer. This work has shown that a jaw phase offset of 1.1 mm can compensate the linear polarization tilt angle offset of 6° found between the polarimeter and the measured values from the RASOR. The source of this discrepancy is still under investigation. In addition, a small amount of beam contamination has been found through the above polarization measurements. The measurement further verifies the theoretical calculation for the APPLE II undulator symmetry mode operation in the soft X-ray range, and it also proves the importance of complete polarization analysis for polarization-sensitive experiments. Polarization measurements will be carried out when the two I10 undulators are working simultaneously so that the polarization state can be monitored *in situ* in the fast polarization switching mode, and in the future the polarization performance for other APPLE II beamlines and undulators will also be checked.

References

Bahrdt, J., Follath, R., Frentrup, W., Gaupp, A. & Scheer, M. (2010). *AIP Conf. Proc.* **1234**, 335–338.

Bahrdt, J., Frentrup, W., Gaupp, A., Scheer, M., Gudat, W., Ingold, G. & Sasaki, S. (2001). *Nucl. Instrum. Methods Phys. Res. A*, **467–468**, 21–29.

Beale, T. A., Hase, T. P., Iida, T., Endo, K., Steadman, P., Marshall, A. R., Dhesi, S. S., van der Laan, G. & Hatton, P. D. (2010). *Rev. Sci. Instrum.* **81**, 073904.

Carr, R., Kortright, J. B., Rice, M. & Lidia, S. (1995). *Rev. Sci. Instrum.* **66**, 1862–1864.

Chubar, O., Elleaume, P. & Chavanne, J. (1998). *J. Synchrotron Rad.* **5**, 481–484.

Drescher, M., Snell, G., Kleineberg, U., Stock, H. J., Muller, N., Heinzmann, U. & Brookes, N. B. (1997). *Rev. Sci. Instrum.* **68**, 1939–1944.

Hirono, T., Kimura, H., Muro, T., Saitoh, Y. & Ishikawa, T. (2005). *J. Electron Spectrosc. Relat. Phenom.* **144–147**, 1097–1099.

Hwang, C. S. & Yeh, S. (1999). *Nucl. Instrum. Methods Phys. Res. A*, **420**, 29–38.

Kimura, H., Hirono, T., Tamenori, Y., Saitoh, Y., Salashchenko, N. N. & Ishikawa, T. (2005). *J. Electron Spectrosc. Relat. Phenom.* **144–147**, 1079–1081.

Kimura, H., Miyahara, T., Goto, Y., Mayama, K., Yanagihara, M. & Yamamoto, M. (1995). *Rev. Sci. Instrum.* **66**, 1920–1922.

Koide, T., Shidara, T., Yuri, M., Kandaka, N., Yamaguchi, K. & Fukutani, H. (1991). *Nucl. Instrum. Methods Phys. Res. A*, **308**, 635–644.

Kortright, J. B. & Underwood, J. H. (1990). *Nucl. Instrum. Methods Phys. Res. A*, **291**, 272–277.

Lidia, S. & Carr, R. (1994). *Nucl. Instrum. Methods Phys. Res. A*, **347**, 77–82.

MacDonald, M. A., Schäfers, F. & Gaupp, A. (2009). *Opt. Express*, **17**, 23290–23298.

Nahon, L. & Alcaraz, C. (2004). *Appl. Opt.* **43**, 1024–1037.

Quitmann, C., Flechsig, U., Patthey, L., Schmidt, T., Ingold, G., Howells, M., Janousch, M. & Abela, R. (2001). *Surf. Sci.* **480**, 173–179.

Sasaki, S. (1994). *Nucl. Instrum. Methods Phys. Res. A*, **347**, 83–86.

Schäfers, F., Mertins, H. C., Gaupp, A., Gudat, W., Mertin, M., Packe, I., Schmolla, F., Di Fonzo, S., Soullié, G., Jark, W., Walker, R., Le Cann, X., Nyholm, R. & Eriksson, M. (1999). *Appl. Opt.* **38**, 4074–4088.

Schmidt, T. & Zimoch, D. (2007). *AIP Conf. Proc.* **879**, 404–407.

Wang, H., Dhesi, S. S., Maccherozzi, F., Cavill, S., Shepherd, E., Yuan, F., Deshmukh, R., Scott, S., van der Laan, G. & Sawhney, K. J. (2011). *Rev. Sci. Instrum.* **82**, 123301.

Wang, H., Dhesi, S. S., Maccherozzi, F. & Sawhney, K. J. S. (2012). *J. Appl. Phys.* **111**, 123117.

Wang, Z., Wang, H., Zhu, J., Zhang, Z., Wang, F., Xu, Y., Zhang, S., Wu, W., Chen, L., Michette, A. G., Pfauntsch, S. J., Powell, A. K., Schafers, F., Gaupp, A., Cui, M., Sun, L. & MacDonald, M. (2007a). *Appl. Phys. Lett.* **90**, 081910.

Wang, Z., Wang, H., Zhu, J., Zhang, Z., Xu, Y., Zhang, S., Wu, W., Wang, F., Wang, B., Liu, L., Chen, L., Michette, G. A., Pfauntsch, J. S., Powell, A. K., Schafers, F., Gaupp, A. & MacDonald, M. (2007b). *Appl. Phys. Lett.* **90**, 031901.

Wang, H., Zhu, J., Wang, Z., Zhang, Z., Zhang, S., Wu, W., Chen, L., Michette, A. G., Powell, A. K., Pfauntsch, S. J., Schäfers, F. & Gaupp, A. (2006). *Thin Solid Films*, **515**, 2523–2526.

Weiss, M. R., Follath, R., Sawhney, K. J. S., Senf, F., Bahrdt, J., Frentrup, W., Gaupp, A., Sasaki, S., Scheer, M., Mertins, H. C., Abramsohn, D., Schäfers, F., Kuch, W. & Mahler, W. (2001). *Nucl. Instrum. Methods Phys. Res. A*, **467–468**, 449–452.

Young, A. T., Arenholz, E., Marks, S., Schlueter, R., Steier, C., Padmore, H., Hitchcock, A. & Castner, D. G. (2002). *J. Synchrotron Rad.* **9**, 270–274.